OPEN ACCESS

University of BRISTOL

Peer reviewed version

University of Bristol - Explore Bristol Research

General rights

Magnetic Surfactants as Molecular Based-Magnets with Spin Glass-Like Properties

Paul Brown[a]*, Gregory N. Smith[b], Eduardo Padrón Hernández[c], Craig James[d], Julian Eastoe[e], Wallace C. Nunes[f], Charles M. Settens[g], T. Alan Hatton[a], Peter J. Baker[h]*.

[a]*Department of Chemical Engineering, Massachusetts Institute of Technology, Cambridge, MA 02139, USA, [b]Department of Chemistry, University of Sheffield, Brook Hill, Sheffield, S3 7HF, UK, [c]Departamento de Física, Universidade Federal de Pernambuco, Recife, Pernambuco, Brazil, [d]CSGI, University of Florence, via della Lastruccia 3 - Sesto Fiorentino, 50019 Florence, Italy, [e]School of Chemistry, University of Bristol, Bristol BS8 1TS, UK, [f]Department of Materials Science and Engineering, Massachusetts Institute of Technology, 77 Massachusetts Avenue, Cambridge, MA 02139, USA, [g]Center for Materials Science and Engineering, Massachusetts Institute of Technology, 77 Massachusetts Avenue, Cambridge, MA 02139, USA, [h]ISIS-STFC, Rutherford Appleton Laboratory, Chilton, Oxon OX11 0QX, UK.

*Corresponding authors e-mail: *peter.baker@stfc.ac.uk, p_brown@mit.edu*

Abstract

This paper reports the use of muon spin relaxation spectroscopy to study how the aggregation behavior of magnetic surfactants containing lanthanide counterions may be exploited to create spin glass-like materials. Surfactants provide a unique approach to building in randomness, frustration and competing interactions into magnetic materials without requiring a lattice of ordered magnetic species or intervening ligands and elements. We demonstrate that this magnetic behavior may also be manipulated via formation of micelles rather than simple dilution, as well as via design of surfactant molecular architecture. This somewhat unexpected result indicates the potential of using novel magnetic surfactants for the generation and tuning of molecular magnets.

Introduction

Molecular-based magnets are a broad class of magnetic materials in which the interactions between magnetic moments are mediated by molecules. They have attracted much interest due to facile modulation of their magnetic properties using organic synthetic methodology processable at room temperature [1, 2] combined with potential applications including organic spintronics. [3] Most molecule-based magnetic systems arrange their magnetic ions in regular structures leading to ferro-, antiferro- and occasionally ferrimagnetism. However, some of them possess metastable frustrated states which may be described as spin glasses [4, 5]. Spin glasses are a class of compound with random interactions between the metal atoms leading to randomly aligned magnetic spins. Above the spin glass transition they behave similarly to paramagnets, but below it their random spin directions do not vary with the time scales associated with laboratory experiments, but remain fixed or rearrange slowly with time. This requires the abandonment of any crystal structure and significant alterations in short-range magnetic interactions in order to form metallic glasses.

A variety of molecular magnets that exhibit spin glass-like behavior can be found in the literature. The linear chain electron transfer salt $[Fe(C_5Me_5)_2][TCNE]$ (TCNE=tetracyanoethylene) [6] was shown to be ferromagnetic at 4.8 K and later, Miller *et al*. demonstrated that $V[TCNE]_x$ was ferromagnetic at room temperature, indicating potential technological use. [7] Both compounds exhibit spin glass-like behavior, where they are weakly disordered but they are not properly glassy. Single molecular magnets offer another route to disordered low-temperature states, an example being the superparamagnetism of Mn12 [8]. In a canonical spin glass it should be possible to alter the concentration of the magnetic moments. Though this is partially achieved for $V[TCNE]_x$ by adding solvent (acetonitrile) to replace TCNE, breaking local symmetry and introducing random anisotropy [9], it is still difficult to tune the distance and interaction strength between the magnetic ions. The process of reversible reabsorption of water to control the magnetic properties of polymeric magnets, sometimes achieving glassy behavior, has led to them being referred to as 'magnetic sponges' [10]. Many other analogous ligands have also been investigated [11], with Miller et al. demonstrating proper spin glass behavior with ethyl tricyanoethylene carboxylate (MeTCEC) [12].

This paper reports the use muon spin relaxation (μSR) spectroscopy [13] to reveal the spin freezing process and spin glass-like behavior of a new magnetic surfactant with a lanthanide counterion [14], 1-decyl-3-

methylimidazolium tetrachloroholminate ([C_{10}mim][HoCl$_4$], Figure 1). Employing a surfactant in this way provides a facile method to prepare a neat solid amorphous sample (a structural glassy state). However, their use also presents an extra curiosity. Surfactants form lyotropic mesophases. That is to say, they self-assemble in a suitable solvent due to their amphiphilicity. Phase formation is controlled by surfactant concentration and molecular architecture as well as choice of solvent. In this paper, a 0.04M micellar solution (micelles are aggregates of surfactants of colloidal dimensions, in this case prolate spheroids with semi-axes a = 25 Å, b = c = 10.4 Å, [14] for a schematic representation see Figure S6 inset) is investigated with the intention of creating islands of magnetic material as a new paradigm for generating molecular-based materials displaying cooperative magnetic behaviour. To-date the only other colloidal approach has involved the synthesis of nanoparticles below the superparamagnetic size limit which act as individually responding magnetic entities [15]. Size and surface effects are important in controlling magnetic properties in both the micellar systems reported herein and nanoparticles [16 - 18], however, micelles offer a much easier route to controlling anisotropy.

In addition, the exchange of an *f*-block metal counterion for a *d*-block counterion was considered by studying the low temperature magnetic behavior of an iron-based surfactant [19], didodecyldimethylammonium tetrachloroferrate (DDAF, Figure 1).

The value in studying these compounds is the huge range of potential surfactants and lipids (ionic, coordinated, covalently bound, organic) that may be used [20]. In addition, the self-aggregation of these compounds in solution into micelles or microemulsions [16], or adsorption on various nanomaterials [21] and biomolecules [22] offers exciting possibilities to provide new methods in designing tuneable nanomagnets. An understanding of the magnetism in these new molecular magnets is important in generating a broad class of molecular-based materials. Muons are ideal to study this phenomenon, as they are able to probe slowly fluctuating systems with a wide fluctuation rate spectrum. [23]
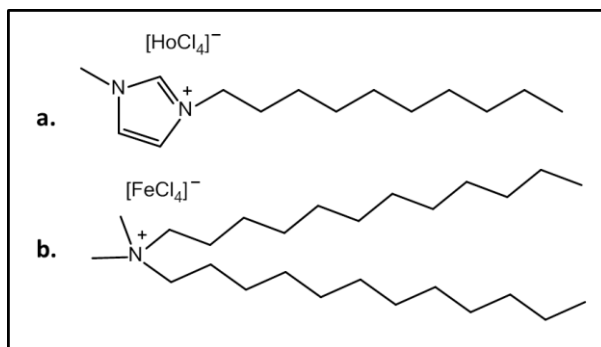
Figure 1: Surfactants studied; a) 1-decyl-3-methylimidazolium tetrachloroholminate [C_{10}mim][$HoCl_4$], and b) didodecyldimethylammonium tetrachloroferrate (DDAF).

Experimental

Materials and Synthesis

Didodecyldimethylammonium chloride (DDAB, >98%) was purchased from TCI Chemicals. 1-decyl-3-methyl imidazolium chloride ([C_{10}mim]Cl, 96%), iron (III) trichloride (99.99%) and holmium chloride hexahydrate (99.9%), were purchased from Sigma Aldrich and used without further purification. Didodecyldimethylammonium tetrachloroferrate (DDAF) was synthesized according to literature [19] by stirring didodecyldimethylammonium chloride with an equimolar amount of iron (III) chloride in methanol overnight. The solvent was removed under reduced pressure and the residue dried *in vacuo* at 80 °C overnight. 1-decyl-3-methyl imidazolium tetrachloroholminate ([C_{10}mim][$HoCl_4$]) was also synthesized according to literature [14], whereby 1 eq. of metal chloride was added to a methanolic solution of [C_{10}mim]Cl and stirred overnight at room temperature, then dehydrated *in vacuo* at 80 °C for 48 hours. The resulting product is a putty-like substance.

SQUID Magnetometry

Magnetic susceptibility data were collected for dried surfactant samples, placed in sealed polypropylene tubes and mounted inside a plastic drinking straw for measurements in a magnetometer equipped with a superconducting quantum interference device (SQUID, MPMS XL-5, Quantum Design, San Diego, USA) and reciprocating sample option (RSO). After demagnetizing at 298K, the samples were cooled in zero field to 5K. The data were then collected in 500 Oe from 5 to 300K at 2K/min. For AC

measurements the samples were zero field cooled (ZFC) and measurements were taken every 0.25 K from 4 K to 18 K as a 5 frequencies between 2 and 1500 Hz.

Muon Spectroscopy

The muon spectroscopy measurements [24, 25] were made on the EMU (8-300K) and MuSR (1.4-20K) instruments at the ISIS Facility, Rutherford Appleton Laboratory, UK. The samples were enclosed in a titanium sample holder (dia. 24mm) with a 30μm Ti window for the muons to pass through before entering the sample. Two types of muon experiments were carried out on the sample as a function of temperature: in zero magnetic field (ZF, <1μT) to examine the unperturbed magnetic behaviour and in a weak field perpendicular to the initial muon spin direction (with transverse field (wTF), 2mT on MuSR, 10mT on EMU) to determine how much of the sample enters a static magnetic state.

For [C_{10}mim][$HoCl_4$] the ZF asymmetry data, $A(t)$, were analyzed using a stretched exponential relaxation that is capable of describing the data over the whole measured temperature range:

$$A(t) = A_s e^{-(\lambda t)^\beta} + A_{bg} \tag{1}$$

where A_s is amplitude of the sample signal, λ is the muon spin relaxation rate, β is the stretching parameter, and A_{bg} is the amplitude of the background signal.

For DDAF the form of the ZF data at low temperature was different. Two distinct relaxing components were apparent and the data were analyzed using the function:

$$A(t) = A_1 e^{-\lambda t} + A_2 e^{-\eta t} + A_{bg} \tag{2}$$

where the first term describes the fast relaxation from muons precessing incoherently in spontaneous local fields perpendicular to their spin direction and the second term describes the relaxation of muon spins due to spin-lattice processes. At higher temperatures the DDAF data took a Gaussian form with a relaxation rate σ.

An 0.04 M aqueous (micellized) solution of [C$_{10}$mim][HoCl$_4$] (2.12g in 100 mL water) was also investigated by first freezing the sample rapidly in liquid nitrogen and cooling the sample down quickly to base temperature in the cryostat. The zero field data take a simple exponential form throughout the temperature range studied:

$$A(t) = A_s e^{-\lambda t} + A_{bg}. \tag{3}$$

For all three samples the wTF (weak Transverse Field) data were analysed in terms of a damped oscillation and a Gaussian relaxation, describing the weakly and strongly magnetic regions of the sample respectively:

$$A(t) = A_{osc} e^{-\Lambda t} \cos(\gamma_\mu B t - \phi) + A_G e^{-\frac{\sigma^2 t^2}{2}} \tag{4}$$

where A_{osc} is the amplitude of the oscillatory term, A_G is the amplitude of the Gaussian term, Λ and σ are muon spin relaxation rates, and φ is the phase of the oscillation. The purpose of the wTF measurements is to compare the fields the muons experience inside the sample with the small field applied perpendicular to the muon spin. The muons precess around the sum of the internal field perpendicular to their spin direction and the applied field. If the muons implant in a weakly magnetic region their precession will be observed. If they implant in a strongly magnetic region they do not contribute to the precession at approximately the applied field because they either undergo rapid spin relaxation due to fluctuating fields along their spin direction or precess rapidly about large static fields. By examining the amplitude of the precession at approximately the applied field, corresponding to muons in weakly magnetic environments, the proportion of the sample that is strongly magnetic can be estimated.

X-Ray Diffraction (XRD)

X-ray powder diffraction (XRD) data was collected using CuK$_\alpha$ radiation on a Rigaku Smartlab multipurpose diffractometer in Bragg-Brentano geometry with a linear position sensitive detector. The sample preparation consisted of pressing the putty-like sample flat on a silicon zero background plate. Analysis of the powder diffraction pattern included indexing to determine the P 12/c1 space group and performing a Pawley extraction procedure of the observed

Bragg peaks. The Rietveld refinement was performed to yield a monoclinic unit cell of a: 7.863Å, b: 6.490Å, c: 12.009Å; $\alpha=\gamma=90°$, $\beta=127.108$.

Small-Angle X-Ray Scattering (SAXS)

Samples were simply placed in a 0.7 mm quartz capillary and measurements recorded with a Rigaku SmartLab XRD multipurpose diffractometer using a sealed-tube CuK_α source with a wavelength of 1.54 Å. The scattering pattern covered scattering vectors ranging from 0.021-0.711 $Å^{-1}$.

Results and Discussion

The magnetic surfactants were prepared via metathesis of the appropriate metal chloride and quaternary alkyl halide. This approach is universally applicable to all cationic surfactants and may also be adopted for anionic surfactants. On drying the sample an amorphous solid was generated as proven by small-angle X-ray scattering (SAXS). SAXS of the solid sample over the range 0.6–100 nm produced no change in intensity above a flat background, representing no long range structure or nanoscale heterogeneity. X-ray diffraction shows a small degree of crystallinity (Figure S1 and S2). Mass spectrometry proved the presence of the $[HoCl_4]$ anion, ESI-MS: m/z 306.8027 [M$^-$, theoretical = 306.7420] .

Magnetic Properties of the Bulk Surfactants Studied via SQUID Magnetometry

From SQUID magnetometry data it is clear that both compounds display simple paramagnetic behaviour at room temperature (Figure 2 and Figure S3). $[C_{10}mim][HoCl_4]$ has a molar susceptibility of 8.55 emu K mol^{-1} Oe^{-1} and effective magnetic moment of 8.30 μ_B This value is lower than the theoretical spin-only values (Ho^{3+} has the $^5I_8$ electronic ground state, with the predicted effective magnetic moment, g[J(J+1)]$^{1/2}$ giving 10.61 μ_B).

$[C_{10}mim][HoCl_4]$ exhibits a reduction in effective magnetic moment (X_mT) on decreasing temperature. No phase transition was observed above 5 K as indicated by a plot of $1/\chi_m$ as a function of temperature (Figure 2), which is linear. The calculated Curie-Weiss value (θ_{cw}) of 2.78 K gives an approximate upper bound on the possible ordering temperature. A full plot of magnetization as a function of field for the solid sample at 2K (Figure S4) supports this conclusion as no hysteresis was observed. DDAF has a molar susceptibility of

3.45 emu K mol^{-1} Oe^{-1} equal to an effective magnetic moment of 5.25 μ_B (Figure 2) similar to literature values, lying close to the values expected for high-spin d^5 Fe^{III} ions (spin-only value: 5.92 μ_B). [26] It obeys the Curie-Weiss law down to 5K and has a θ_{cw} = -6.63 K, suggesting that antiferromagnetic interactions dominate. It has previously been reported that in metal salts of this kind 3-dimensional ordering can occur at low temperature through superexchange coupling via two diamagnetic intermediaries [27].
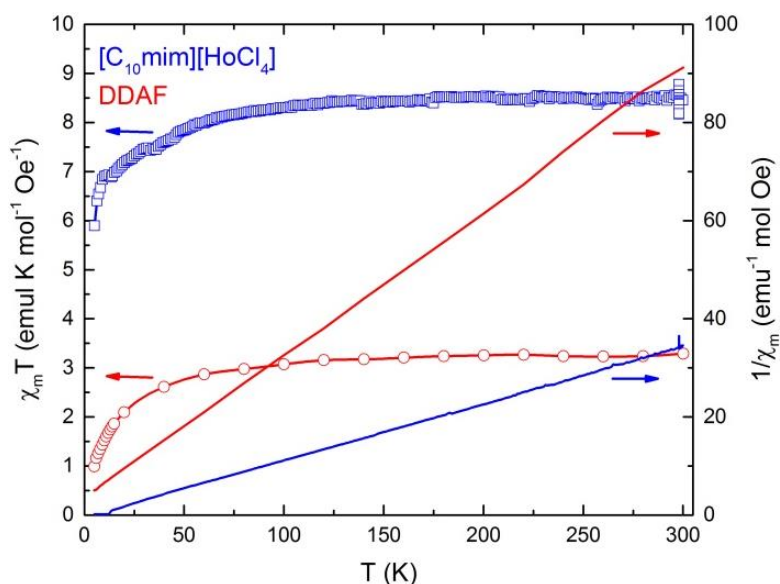
Figure 2: SQUID magnetometry data showing molar magnetic susceptibility as a function of temperature, χ_mT, for [C$_{10}$mim][HoCl$_4$] and DDAF (symbols), and a Curie-Weiss plot, 1/χ_m vs T (lines).

It was clear from Figure 1 and S3 that there is a transition at around 12 K for [C$_{10}$mim][HoCl$_4$]. AC susceptibility measurements were taken to investigate further. Real (χ') and imaginary (χ'') components of magnetization were taken as a function of temperature (4 - 18K at 0.25 K intervals) and at several frequencies (2 Hz – 1500 Hz, Figure 3). In a zero field cooled (ZFC) sample no cusp (indicating a freezing temperature) was observed in the χ' vs temperature data. Typically, the frequency dependence of such a cusp would be evidence of a spin-glass transition [28]. However, a frequency dependence of χ' was observed below 14 K with a slight bump at around 12 K, see Figure 3. These results can be related to the occurrence of frozen magnetic effect involving a fraction of the magnetic moments of the sample (χ'' was too weak to be successfully analysed).
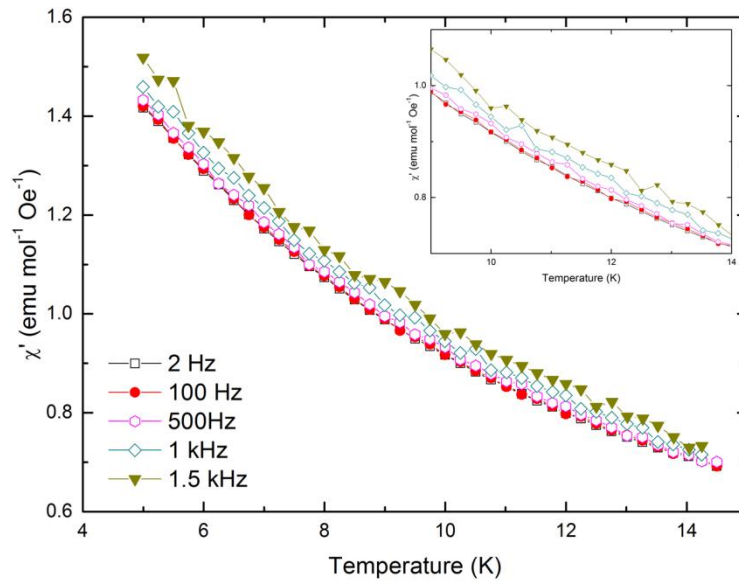
Figure 3: Plot of the real component of magnetization (χ') as a function of temperature.

Muon Spin Relaxation Measurements of Bulk [C$_{10}$mim][HoCl$_4$]

The results of the muon spin relaxation experiments on [C$_{10}$mim][HoCl$_4$] are shown in Figure 4. Panel (a) shows the ZF (zero magnetic field) asymmetry data as a function of temperature. It is notable that the initial asymmetry is around 16%, rather than the ~23% expected for the instrument if measuring a material such as Ag where no muonium is formed and the magnetic moments present are very small. We also measured a non-magnetic control sample, DDAB, where the initial asymmetry is similar. Furthermore, the trends in zero and transverse field parameters mirror each other. From this it may be concluded that around one third of the muons form muonium states in this sample; this appears to be constant over the measured temperature range and appears to make no further alteration to the signal. Both the relaxation rate (λ) and the shape of the relaxation (β) change with temperature and are shown in panel (c). At the highest measured temperatures the value of β approaches 2, as would be expected from the Gaussian distribution of fields due to nuclear moments in the sample. Any fields from electronic moments will be fluctuating on too short a timescale for the muons to be sensitive to them. As the temperature is lowered the electronic moment fluctuations slow down and enter the time window over which muons are sensitive (roughly MHz – THz). There is crossover between the high temperature Gaussian relaxation and the approximately square root exponential relaxation below 10 K. Values of $\beta<1$ are typical for broadened field distributions such as those in spin glasses [29]. The relaxation rate λ grows slowly with cooling to 20 K and then much more rapidly below 10 K, coincident with the transition observed in the AC magnetometry.
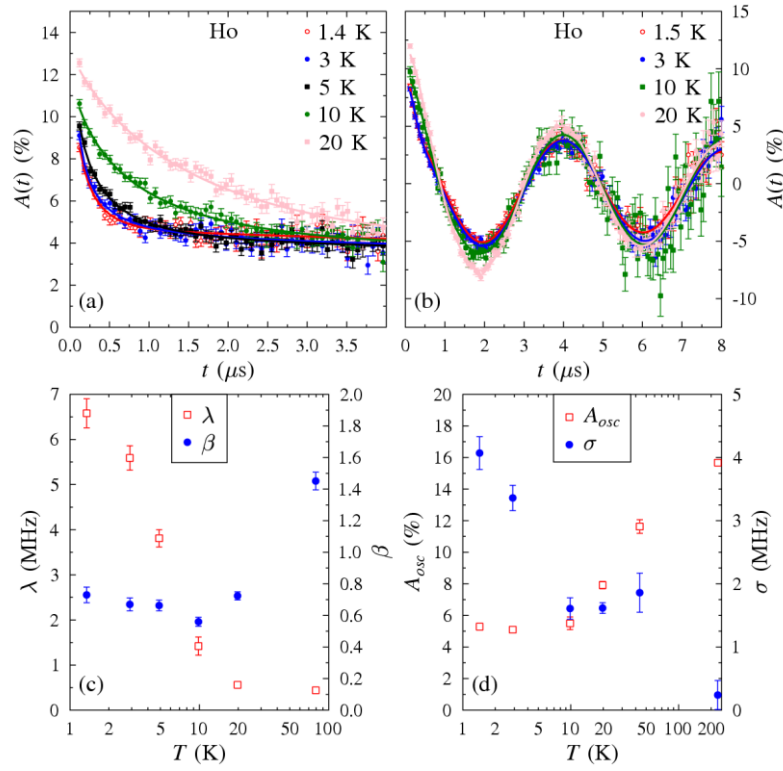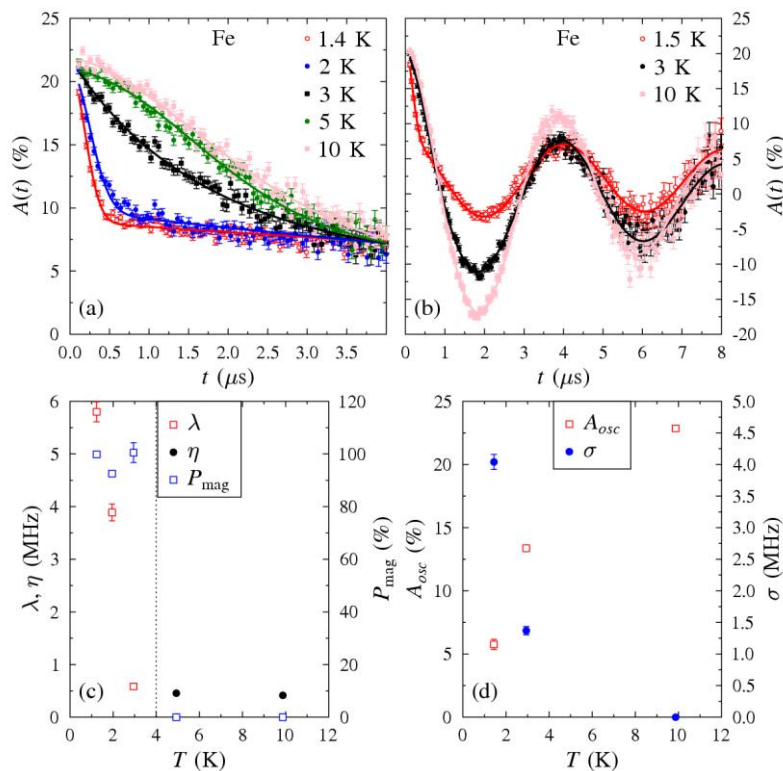
Figure 4: Muon decay asymmetry spectra and fitted parameters for [C$_{10}$mim][HoCl$_4$]. (a) Zero field data. (b) Weak transverse field data. Solid lines show the best fitted relaxation function. (c) Zero field parameters. (d) Weak transverse field parameters.

In the raw wTF data shown in Figure 4b the significant changes occur in the first 2µs as a Gaussian relaxation component increases in relaxation rate, σ, and amplitude. The slowly relaxing co-sinusoidal component of the asymmetry shows a corresponding decrease in amplitude at low temperature, complete below 10K. The static magnetic volume fraction can be estimated from the relative amplitude of the A_S term in the low-temperature magnetic and paramagnetic phases, here 5.2% and 15.7% respectively. Since the low temperature value is close to the background level seen in ZF it may be concluded that there is strong magnetism influencing practically all muon stopping sites. Returning to the zero field data, the limiting value of β = 1/3 as the T_g is approached is a general finding for a significant number of spin-glass systems [30 - 32]. Combining the ZF and wTF data there is local evidence that [C$_{10}$mim][HoCl$_4$] enters a spin-glass-like state at around 10 K [23]. This is the case throughout the sample volume and agrees well with the AC magnetometry described above. The internal fields can be estimated from the relaxation rates to be around 50mT ($B_{loc} \sim \lambda/\gamma_\mu$).

Muon Spin Relaxation Measurements of Bulk DDAF

Figure 5 shows the muon data and fitted parameters for DDAF. In panel (a) a change is evident in the ZF data around 3K and this is replicated in the wTF data shown in panel (b). Above 5K the ZF data take a Gaussian form as would be expected in a paramagnetic system where the electronic magnetic moments fluctuate rapidly and muon spins are depolarized by quasistatic fields from nuclear magnetic moments [23]. Below 3 K two components are evident in the ZF data. The parameters derived from fitting the ZF data are shown in panel (c). The Gaussian relaxation at high temperature appears close to temperature independent (consistent with higher temperature data recorded using EMU). Below ~4 K the relaxation rate λ increases with decreasing temperature. It may be estimated that the (short-range) ordered magnetic volume fraction using the relative size of the two components A_1 and A_2 as $P_{mag} = 1.5*A_1/(A_1+A_2)$. This expression follows from the geometrical averaging of fields perpendicular ($2/3^{rds}$) or parallel ($1/3^{rd}$) to the muon spin direction and the expectation that the relaxation rate in paramagnetic volumes will be significantly smaller than in statically magnetic ones. The magnetic volume fraction thus derived is $100 \pm 2\%$.

In the wTF data a similar drop in the oscillating asymmetry is observed, going through the transition around 3 K to that observed in [C_{10}mim][$HoCl_4$] around 10K, with the relative amplitudes at low (6%) and high temperature (21%). The relaxation rate σ grows rapidly below the transition and has a similar magnitude to that observed in the Ho sample.

Figure 5: Muon decay asymmetry spectra and fitted parameters for DDAF. (a) Zero field data. (b) Weak transverse field data. Solid lines show the best fitted relaxation function. (c) Zero field parameters. (d) Weak transverse field parameters.

Muon Spin Relaxation Measurements of [C$_{10}$mim][HoCl$_4$] upon Micellization

To investigate the effect of micelle formation on the magnetic properties of [C$_{10}$mim][HoCl$_4$] a 0.04 M micellar solution was selected. This value is slightly above the critical micelle concentration (cmc = 0.030 M) meaning that 75% of surfactant molecules exist as free monomers in solution. It has been estimated in literature [14] via small-angle neutron scattering (SANS) that the micelles that do exist are ellipsoidal with a volume of around 11 nm^3 (Figure S6) and from electrical conductivity that around 80% of the counterions make up the Stern layer (the double layer of ions screen the positively charged micelle surface), thus forming "magnetic islands".

For this sample we focus on data recorded on the EMU instrument between 8 and 250 K (Figure 6). Lower temperature measurements were recorded on MuSR down to 1.4 K but the parameters follow the higher temperature trends without any further transitions. The most significant changes in the micellar solution are evident in the weak transverse field data around 100 K, with a drop in the relaxing asymmetry from the high temperature value of ~10% to ~6%. This suggests that muons in approximately 40% of the sample

experience significant static (disordered) magnetic fields. Accompanying this drop in the relaxing asymmetry is an increase in the distribution of internal fields parameterized by the relaxation rate, σ. Because only part of this sample becomes magnetic the zero field results (fitted with $\beta=1$) are less instructive than for the concentrated samples but a distinct drop in the initial asymmetry on cooling is seen, that mirrors that observed in the weak transverse field.

Since the volume occupied by the micelles at this concentration is very small, ~0.4 vol%, it is apparent that the magnetic fields experienced by the muons must extend well beyond the micelles at even 100 K, beyond the range that dipolar fields seem plausible to explain the data. Most of the surfactant molecules remain in the solution rather than in the micelles so it seems possible that some magnetic polarization of molecules in the frozen solution occurs to increase the volume of the strongly magnetic regions of the sample. The proportion of the sample apparently magnetic is lower than in the undiluted sample but the onset temperature of the effect is far higher. On the basis of the present data a conclusive explanation is not possible and this suggests further study of this question using other techniques would be worthwhile.
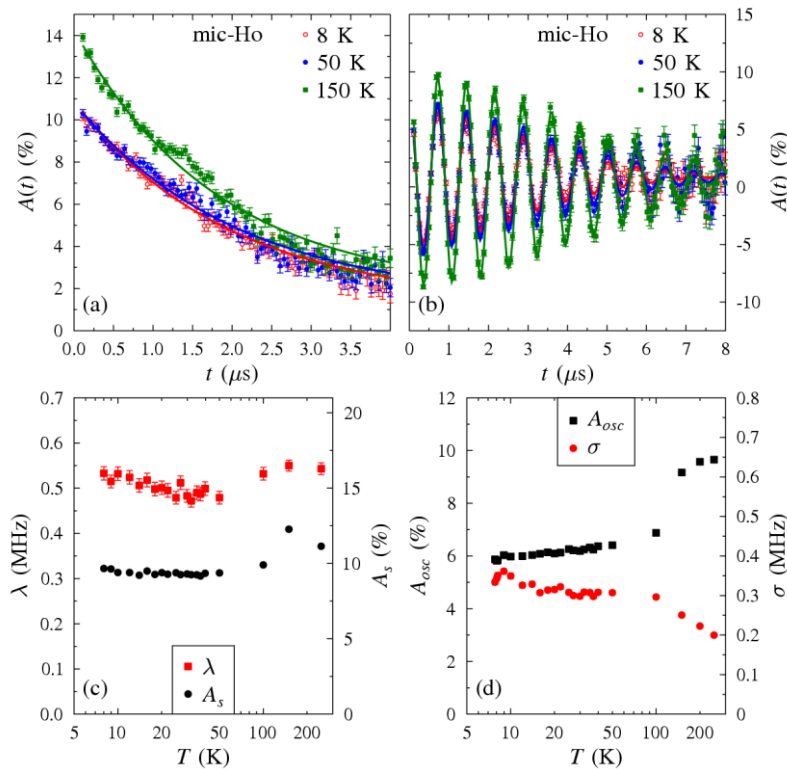
Figure 6: Muon decay asymmetry spectra and fitted parameters for 0.04M micellar [C_{10}mim][$HoCl_4$]. (a) Zero field data. (b) Weak transverse field data. Solid lines show the best fitted relaxation function. (c) Zero field parameters. (d) Weak transverse field parameters.

Conclusions

Muon spin relaxation spectroscopy and SQUID magnetometry have proven useful tools in elucidating the magnetic behavior in a new class of d and f-block metal based ionic surfactants. Specifically, the pure iron-based surfactant, DDAF appears to have quasistatic short-ranged magnetic correlations at low temperatures. However, on selecting a holmium-based surfactant, [C_{10}mim][HoCl$_4$], disordered dynamics are observed indicating spin-glass like behaviour. Interestingly, even a dilute micellar solution of surfactant (0.04 M) demonstrated static magnetism in a weak transverse field as indicated by a drop in relaxing asymmetry. This change occurs at a higher temperature than the pure sample and must extend well beyond the micelle "islands" themselves. We conceptualize the magnetic properties in this solution akin to "magnetic islands" surrounded by "magnetic reefs". In comparison to earlier research [6, 7], no lattice formation is apparent with frustrations and randomness introduced by the surfactant moiety.

These experiments demonstrate that the surfactant nature of the metal salt leads to tunable micelles via change in concentration (control of lyotropic mesophases should also be expected at higher concentrations) unlike previous reports of simple dilution. [7] Also highlighted is that surfactant architecture also has a significant role to play. Only one class of surfactants (cationic) was selected for this study but other classes do exist (chelating, covalently bound etc.) [20] with potentially interesting properties, requiring further investigations. In addition, the ability for these surfactants to adsorb onto surfaces such as nanoparticles etc. [18, 20] may provide alternative routes for developing molecular magnets.

References

1. Metallomesogens, synthesis, properties, and applications, Ed. J. L. Serrano, VCH, **2006.**

2. R. A. Layfield, Organometallic Single-Molecular Magnets, *Organometallics*, **2014**, 33, 1084-1099.

3. J. W. Yoo, H. W. Jang, V. N. Prigodin, C. Kao, C. B. Eom, A. J. Epstein, Giant magnetoresistance in ferromagnetic/organic semiconductor/ferromagnet heterojunctions*, Phys. Rev. B,* **2009**, 80, 205207.

4. J. A. Mydosh, Spin glasses: redux: an updated experimental/materials survey, *Rep. Prog. Phys.,* **2015**, 78, 052501.

5. D. L. Stein, C. M. Newman, Spin Glasses and Complexity, Princeton U. Press, **2013**.

6. J. S. Miller, P. J. Krusic, A. J. Epstein, W. M. Reiff, J. Hua Zhang, Linear Chain Ferromagnetic Compounds – Recent Progress, *Mol. Cryst. Liq. Cryst.,* **1985**, 120, 27-34.

7. J. M. Manriquez, G T. Lee, R. S. McLean, A. J. Epstein, J. S. Miller, A Room-Temperature Molecular/Organic-Based Magnet, *Science,* **1991**, 252, 1415-1417.

8. A. Caneschi, D. Gatteschi, R. Sessoli, A. L. Barra, L. C. Brunel, M. Guillot, Alternating current susceptibility, high field magnetization, and millimeter band EPR evidence for a ground S = 10 state in [Mn12O12(Ch3COO)16(H2O)4].2CH3COOH.4H2O, *J. Am. Chem. Soc*., **1991**, 113, 5873-5874.

9. Y. Lu, H. Yu, M. Harberts, A. J. Epstein, E. Johnston-Halperin, Vanadium[ethyl tricyanoethylene carboxylate]$_x$: a new organic-based magnet, *J. Mater. Chem. C*, **2015**, 3, 7363-7369.

10. O. Kahn, J. Larionova, J. V. Yakhmi, Molecular Magnetic Sponges, *Chem. Eur. J*., **1999**, 5, 3443-3449.

11. P. Zhou, B. G. Morin, J. S. Miller, A. J. Epstein, Magnetization and static scaling of the high-Tc disordered molecular-based magnet V(tetracyanoethylene)x.y(CH3CN) with x~1.5 and y~2, *Phys. Rev. B,* **1993**, 48, 1325.

12. K. I. Pokhodnya, B. Lefler, J. S. Miller, A Methyl Tricyanoethylenecarboxylate-Based Room-Temperature Magnet, *Adv. Mater.*, **2007**, 19, 3281-3285.

13. S. J. Blundell, T. Lancaster, M. L. Brooks, F. L. Pratt, M. L. Taliaferro, J. S. Miller, A µSR study of the metamagnetic phase transition in the electron-transfer salt [FeCp2][TCNQ], *Physica B,* **2006**, 374-375, 114-117.

14. P. Brown, A. Bushhmelev, C. P. Butts, J-C. Eloi, I. Grillo, P. J. Baker, A. M. Schmidt, J. Eastoe, Properties of New Magnetic Surfactants, *Langmuir*, **2013**, 29, 3246-3251.

15. X. Battle, A. Labarta, Finite-size effects in fine particles: magnetic and transport properties, *J. Phys D*, **2002**, 35, R15-R42.

16. P. Brown, C. P. Butts, J. Eastoe, S. Glatzel, I. Grillo, S. H. Hall, S. Rogers, K. Trickett, Microemulsions as tunable nanomagnets, *Soft Matter*, **2012**, 8, 46, 11609-11612.

17. S. Sharma, R. S. Ningthoujam, N. S. Gajbhiye, Spin-glass-like behavior of surfactant capped Co$_{50}$Ni$_{50}$ nanoparticles, *Chem. Phys. Lett*., **2013**, 558, 48-52.

18. S. Kim, C. Bellouard, J. Eastoe, N. Canilho, S. E. Rogers, D. Ihiawakrim, O. Ersen, A. Pasc, Spin State As a Probe of Vesicle Self-Assembly, *J. Am. Chem. Soc.*, **2016**, DOI: 10.1021/jacs.6b00537.

19. P. Brown, A. Bushmelev, C. P. Butts, J. Cheng, Eastoe, I. Grillo, R. K. Heenan, A. M. Schmidt; Magnetic Control over Liquid Surface Properties with Responsive Surfactants, *Angew. Chem. Int. Ed.*, **2012**, 51, 2414-2416.

20. P. Brown, T. A. Hatton, J. Eastoe, Magnetic Surfactants, *Curr. Opin. Coll. Int. Sci.*, **2015**, 20, 140-150.

21. S. Kim, C. Bellouard, A. Pasc, E. Lamouroux, J. Blin, C. Carteret, Y. Fort, M. Emo, P. Durand, M. Stébé, Nanoparticle-free magnetic mesoporous silica with magneto-responsive surfactants, *J. Mat. Chem. C*, **2013**, 42, 6930-6934.

22. P. Brown, A. M. Khan, J. P. Armstrong, A. W. Perriman, C. P. Butts, J. Eastoe, Magnetizing DNA and proteins using responsive surfactants, *Adv. Mater.*, **2012**, 24, 6244-6247.

23. L. Nuccio, L. Schulz, A. J. Drew, Muon spin spectroscopy: magnetism, soft matter and the bridge between the two, *J. Phys. D: Appl. Phys.*, **2014**, 47, 473001.

24. S. J. Blundell, Spin-polarized muons in condensed matter physics, *Contemp. Phys.*, **1999**, 40, 175-192.

25. S. J. Blundell, Muon-Spin Rotation Studies of Electronic Properties of Molecular Conductors and Superconductors, *Chem. Rev.*, **2004**, 104, 5717–5736.

26. D. Moon, J. Kim, M. S. Lah, Synthesis and Characterization of Mononuclear Octahedral Fe(III) Complex Contianing a Biomimetic Tripodal Ligand, N-(Benzimidazol-2-ylmethyl)iminodiacetic Acid, *Bull. Korean. Chem. Soc.,* **2006**, 27, 1597.

27. A. García-Saiz, P. Migowski, O. Vallcorba, J. Junquera, J. A. Blanco, J.A. González, M. T. Fernández-Díaz, J. Rius, J. Dupont, J. R. Fernández, I. de Pedro, A Magnetic Ionic Liquid Based on Tetrachloroferrate Exhibits Three-Dimensional Magnetic Ordering: A Combined Experimental and Theoretical Study of the Magnetic Interaction Mechanism, *Chem. Eur. J.*, **2014**, 20, 72-76.

28. J. A. Mydosh, Spin Glass; An Experimental Introduction, Taylor and Francis, London, **1993**.

29. R. M. Pickup, R. Cywinski, C. Pappas, B. Farago, P. Fouquet, Generalized Spin-Glass Relaxation, *Phys. Rev. Lett.*, **2009**, 102, 097202.

30. I. A. Campbell, A. Amato, F. N. Gygax, D. Herlach, A. Schenk, R. Cywinski, S. H. Kilcoyne, Dynamics in canonical spin glasses observed by muon spin depolarization, *Phys. Rev. Lett.*, **1994**, 72, 1291-1294.

31. S. R. Dunsiger, R. F. Kiefl, K. H. Chow, B. D. Gaulin, M. J. P. ingras, J. E. Greedan, A. Keren, K. Kojima, G. M. Luke, W. A. MacFarlane, N. P. Raju, J. E. Sonier, Y. J. Uemura, W. D. Wu, Muon spin relaxation investigation of the spin dynamics of geometrically frustrated antiferromagnets $Y_2Mo_2O_7$ and $Tb_2Mo_2O_7$, *Phys. Rev. B*, **1996**, 54, 9019-9022.

32. J. R. Stewart, A. D. hillier, S. H. Kilcoyne, P. Manuel, M. T. F. Telling, R. Cywinski, Moment localization in β-MnAl, *J. Mag. Mag. Mater.*, **1998**, 177-181, 602-604.

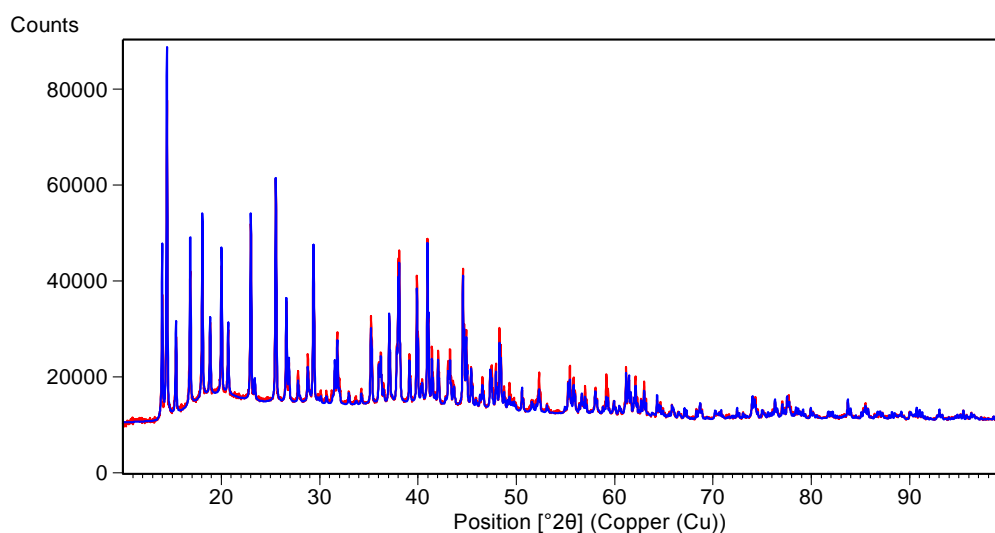# Magnetic Surfactants as Molecular Based-Magnets with Spin Glass-Like Properties

Paul Brown[a], Gregory N. Smith[b], Eduardo Padrón Hernández[c], Craig James[d], Julian Eastoe[e], Wallace C. Nunes[f], Charles M. Settens[g], T. Alan Hatton[a], Peter J. Baker[h].

[a]Department of Chemical Engineering, Massachusetts Institute of Technology, Cambridge, MA 02139, USA, [b]Department of Chemistry, University of Sheffield, Brook Hill, Sheffield, S3 7HF, UK, [c]Departamento de Física, Universidade Federal de Pernambuco, Recife, Pernambuco, Brazil, [d]CSGI, University of Florence, via della Lastruccia 3 - Sesto Fiorentino, 50019 Florence, Italy, [e]School of Chemistry, University of Bristol, Bristol BS8 1TS, UK, [f]Department of Materials Science and Engineering, Massachusetts Institute of Technology, 77 Massachusetts Avenue, Cambridge, MA 02139, USA, [g]Center for Materials Science and Engineering, Massachusetts Institute of Technology, 77 Massachusetts Avenue, Cambridge, MA 02139, USA, [h]ISIS-STFC, Rutherford Appleton Laboratory, Chilton, Oxon OX11 0QX, UK.

Figure S1: X-Ray Diffraction pattern of $[C_{10}mim][HoCl_4]$ and, in blue, the calculated pattern (.CIF file included in supporting information)
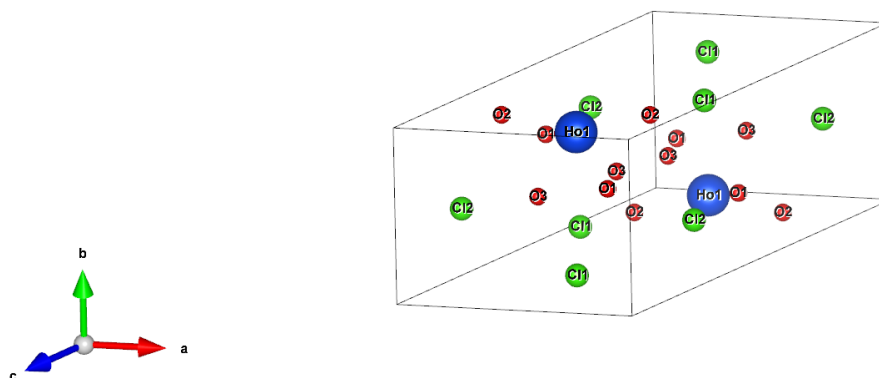
Figure S2: Crystal structure of $[C_{10}mim][HoCl_4]$ corresponding to the calculated pattern from Rietveld refinement.
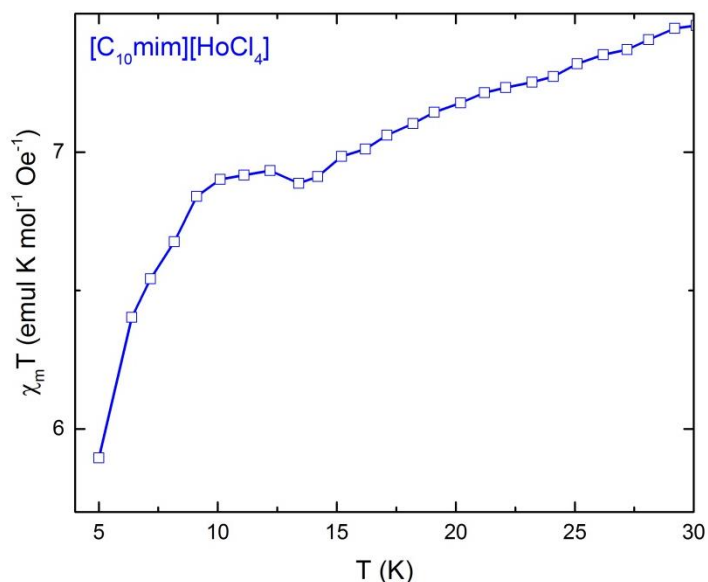
Figure S3: SQUID magnetometry data showing molar magnetic susceptibility as a function of temperature (5 – 30 K), $\chi_m T$, for [C$_{10}$mim][HoCl$_4$].
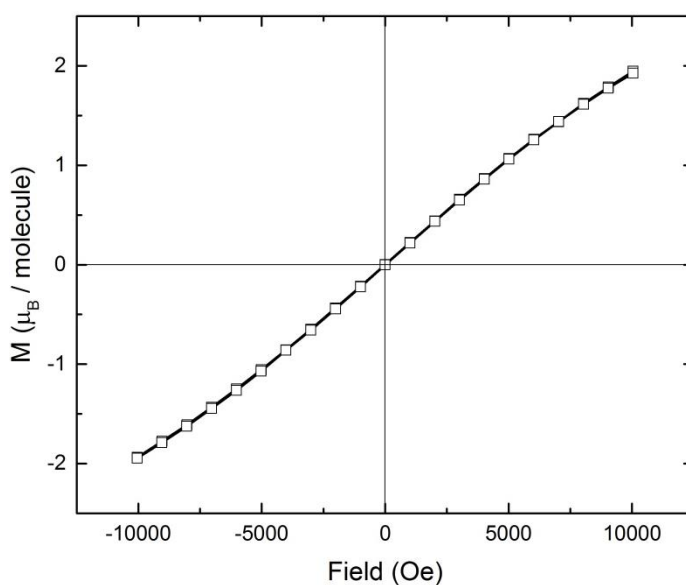
Figure S4: Full hysteresis slope for [C$_{10}$mim][HoCl$_4$] at 5K.

Small-Angle Neutron Scattering (SANS)

Scattering was measured on the D22 diffractometer at ILL, Grenoble, France. D22 is a reactor-based diffractometer, and a neutron wavelength of $\lambda = 10$ Å was employed at two different detector distances, giving $0.0024 < Q < 0.37$ Å^{-1}. Appropriate normalization using site-specific procedures gave the absolute cross section $I(Q)$ (cm^{-1}) as a function of momentum transfer Q (Å^{-1}). Measurements of the dilute aqueous

system was carried out in D$_2$O (scattering length density $\rho = 6.33 \times 10^{10}$ cm^{-2}) to provide the necessary contrast, and the sample was placed in a Hellma fused silica cuvette with a path length of 2 mm. Raw SANS data was normalized by subtracting the scattering of the empty cell and a solvent background using appropriate transmission measurements. Any low level of residual incoherent scattering was accounted for by a flat background term during the fitting process.

SANS Scattering Laws and Model Fitting

Scattering intensity *I(Q)* is linked to the size and shape of the aggregates (form factor, *P(Q)*) and the interaction between these aggregates (structure factor, S(Q)),

$$I(Q) \propto P(Q, R)S(Q) \qquad\qquad\qquad \text{Eq. S1}$$

where *R* is the particle radius.

SAS-View was used to fit the data. The surfactant was fitted using a hard sphere structure factor (*HSS(Q)*),[1] fitting to parameters of R_a (radius equatorial) and R_b (radius polar) (*c.f.* Figure S6 inset) as well as the hard sphere volume fraction, HSϕ.

Here, $R_a = 24.96$ Å and $R_b = 10.4$ Å.
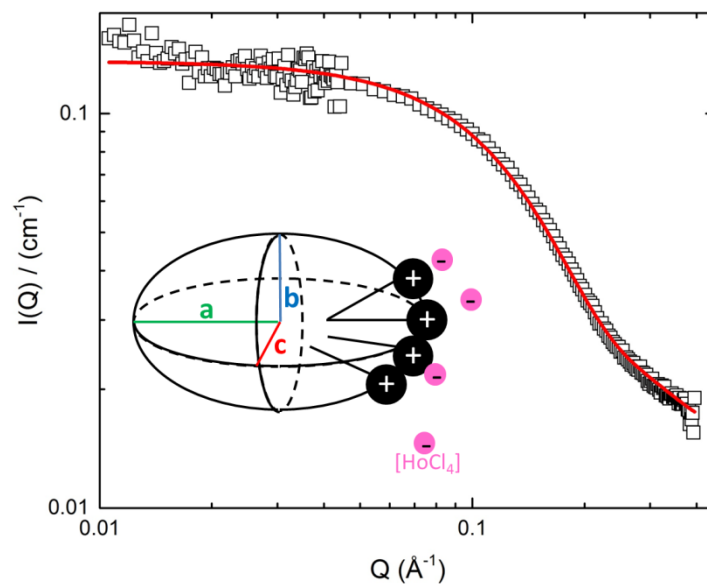
Figure S6: SANS profile for a 0.04 M aqueous micellar solution of $[C_{10}mim][HoCl_4]$. Line through data is a fit using a model for a charged ellipsoidal micelle with a hard sphere structure factor (HSSQ). Inset is a schematic of how the surfactant moieties self-assemble in water to form the micelles.

References

1. Ashcroft, N. W.; Lekner, J. Structure and Resistivity of Liquid Metals *Phys. Rev.* **1966**, *145*, 83-90.